Universität Karlsruhe (TH)
Research University · founded 1825

CRC 461
Strong Earthquakes:
A Challenge for Geosciences and Civil Engineering

Low−frequency limit for H/V studies due to tilt

Thomas Forbriger

Geophysical Institute, University of Karlsruhe
and
Black Forest Observatory (BFO)
Research facility of the Universities of Karlsruhe and Stuttgart, Heubach 206, D−77709 Wolfach

1 Low-frequency H/V peak

Throughout the data recorded during the URS project (Ritter *et al.* 2005) in Bucharest city, we observe a low-frequency peak in H/V ratio near 0.2 Hz (Ziehm 2006). The frequency of this peak systematically varies from lower frequencies in the north to higher frequencies in the south. This variation is believed to be caused by the dipping of the interface between the Neogene and the Cretaceous at a depth from 1000 m to 2000 m. Unfortunately the H/V level below 0.15 Hz is unstable and strongly rises with decreasing frequency in the recordings of most stations. This puts an effective limit on the analysis of the peak at frequencies below 0.2 Hz (Fig. 1). Since in some of the data there appears to be a power-law relation between H/V ratio and frequency below 0.15 Hz, I discuss tilt as a possible cause of this strong increase.

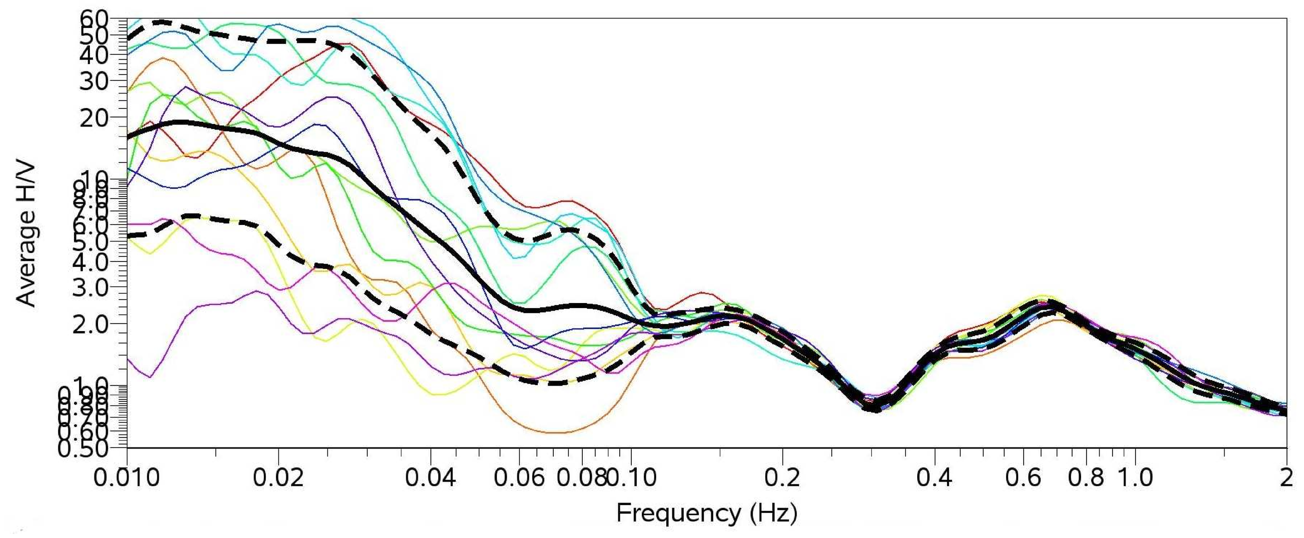

Figure 1: H/V ratio for station URS14. Two peaks (at 0.15 Hz and 0.7 Hz) are apparent. Each thin curve is H/V for a different time window, while the black curve displays the average with the dashed curves marking standard deviation. Courtesy of Julia Ziehm.

2 Forces acting on inertial sensors

Inertial sensors (gravimeters, seismometers and tiltmeters) sense inertial and gravitational acceleration. Due to the equivalence of inertial and gravitational mass they are principally unable to distinguish between both (Wielandt 2002, secs. 2.1 and 3.3). The inertial acceleration in the horizontal direction is

$$a_h = \frac{\partial^2 u_h}{\partial t^2} \quad \text{and} \quad a_z = \frac{\partial^2 u_z}{\partial t^2} \tag{1}$$

in vertical direction, where $u_z(h,z,t)$ is the vertical component of displacement and $u_h(h,z,t)$ the horizontal component. For small tilt angles the horizontal component of a seismometer sitting on the ground additionally senses the acceleration

$$a_\tau \approx g\frac{\partial u_z}{\partial h} \tag{2}$$

due to ground tilt, where g is the gravitational acceleration (Fig. 2).

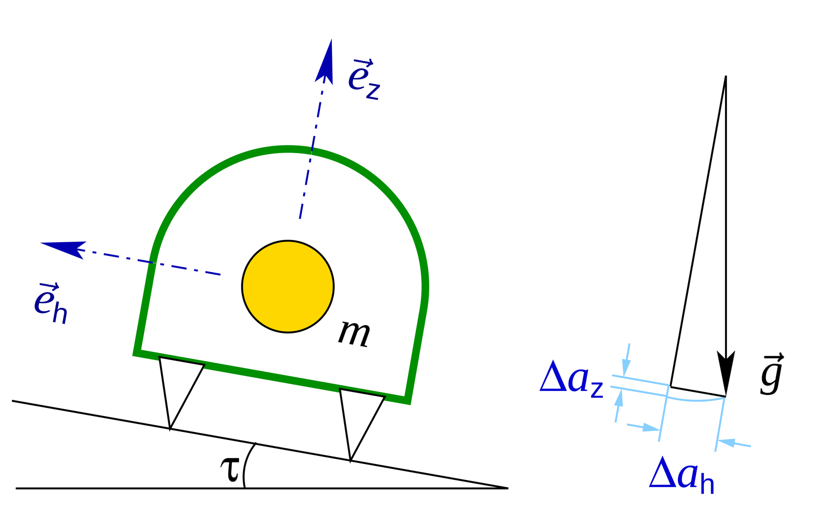

Tilt has a linear contribution

$$\Delta a_h = g\sin(\tau) \approx g\tau \tag{3}$$

to the horizontal component's acceleration while its contribution

$$\Delta a_z = g\,(1-\cos(\tau)) \approx \frac{g}{2}\tau^2 \tag{4}$$

to the vertical component is of second order. For this reason the effect usually is only significant in the horizontal component's signal.

Figure 2: Tilt changes the alignment of the gravitational acceleration $\vec{g}$ to the sensitive directions $\vec{e}_z$ and $\vec{e}_h$ of the seismometer's components. Both experience a change Δa_z and Δa_h in acceleration, respectively.

If $\tilde{a}_z$, $\tilde{a}_h$, and $\tilde{a}_\tau$ are the Fourier transforms of a_z, a_h, and a_τ, respectively, the Fourier transform of the seismometer's vertical component output signal is

$$\tilde{s}_z(\omega) = T(\omega)\tilde{a}_z(\omega), \tag{5}$$

where $T(\omega)$ is the instrument's complex response function. And

$$\tilde{s}_h(\omega) = T(\omega)\,(\tilde{a}_h(\omega) + \tilde{a}_\tau(\omega)) \tag{6}$$

for the horizontal component's output signal.

3 Tilt contribution to H/V ratio

H/V ratio is calculated from seismic recordings usually by

$$A_{\mathrm{H/V}}(\omega) = \frac{|\tilde{s}_h(\omega)|}{|\tilde{s}_z(\omega)|} = \frac{|\tilde{a}_h(\omega) + \tilde{a}_\tau(\omega)|}{|\tilde{a}_z(\omega)|} \tag{7}$$

and averaging over signals from several time windows. Hence the H/V ratio contains a tilt contribution, which may be ignored at high frequencies since the inertial term rises with ω^2. At low frequencies the tilt contribution can dominate $A_{\mathrm{H/V}}$.

4 Point load on an elastic halfspace

The elastic deformation of a homogeneous halfspace due to a static point load is known as the „Boussinesque solution" in the theory of elasticity (Fig. 3). According to Zürn (2003) the solution to Boussinesque's problem is

$$u_z(r,z) = -\frac{F}{4\pi\mu R}\frac{1}{}\left(\frac{\lambda+2\mu}{\lambda+\mu} + \frac{z^2}{R^2}\right) \tag{8}$$

for the vertical component and

$$u_r(r,z) = -\frac{F}{4\pi(\lambda+\mu)}\frac{1}{r}\left(1 + \frac{z}{R} + \frac{\lambda+\mu}{\mu}\frac{r^2 z}{R^3}\right) \tag{9}$$

for the horizontal component. It is given in cylindrical coordinates with the radial coordinate $r = \sqrt{x^2+y^2}$ and the spacial distance $R = \sqrt{r^2+z^2}$ to the load. The loading force at the origin is

$$\vec{f} = -F\delta(\vec{x})\hat{e}_z \tag{10}$$

and λ and μ are Lamé's parameters for the homogeneous halfspace at $z < 0$.

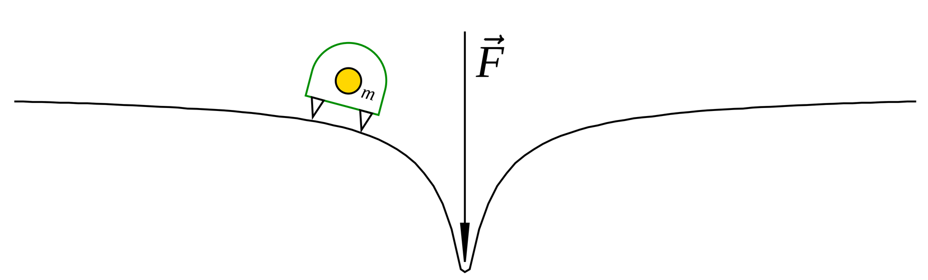

Figure 3: Deformation of a point load on a homgeneous, elastic halfspace (schematically; the deformation would become infinite at the location of the load). This is a model for the seismic near-field of passing vehicles. In the near-field deformation is instantaneous (quasistatic). A seismometer on the surface is tilted.

For observations at the surface of the elastic halfspace I simply obtain

$$u_z(r,z=0) = -\frac{F}{4\pi\mu r}\frac{1}{}\frac{\lambda+2\mu}{\lambda+\mu} \tag{11}$$

for the vertical component and

$$u_r(r,z=0) = -\frac{F}{4\pi(\lambda+\mu)}\frac{1}{r} \tag{12}$$

for the horizontal component, which is valid for $r > 0$.

For $F(t)$ varying with time eqs. (11) and (12) are the near-field solution. In this case the seismometer senses

$$a_z(t,r,z=0) = -\frac{\ddot{F}(t)}{r}\frac{\lambda+2\mu}{4\pi\mu(\lambda+\mu)}, \tag{13}$$

$$a_h(t,r,z=0) = -\frac{\ddot{F}(t)}{r}\frac{1}{4\pi(\lambda+\mu)}, \tag{14}$$

and

$$a_\tau(t,r,z=0) = g\frac{\partial u_z(t,r,z)}{\partial r} \tag{15}$$

$$= g\frac{F(t)}{r^2}\frac{\lambda+2\mu}{4\pi\mu(\lambda+\mu)}. \tag{16}$$

Using eq. (7) I obtain

$$A_{\mathrm{H/V}}(\omega) = \frac{\mu}{\lambda+2\mu} + \frac{g}{r\omega^2} \tag{17}$$

for the effect of the point load in the H/V analysis. While it is constant and less than 1 with

$$\lim_{\omega\to\infty} A_{\mathrm{H/V}}(\omega) = \frac{\mu}{\lambda+2\mu} \tag{18}$$

at high frequencies, its contribution

$$\lim_{\omega\to 0} A_{\mathrm{H/V}}(\omega) = \frac{g}{r\omega^2} \tag{19}$$

is increasing with decreasing frequency.
Consider a point load at $r = 10\,\mathrm{m}$ distance, with $\lambda = \mu$ in the halfspace and $g = 9.81\,\mathrm{m\,s^{-2}}$. Then the tilt contribution is larger than 2 at frequencies less than 0.11 Hz and is likely to mask H/V peaks produced by surface wave ellipticity (Fig. 4).

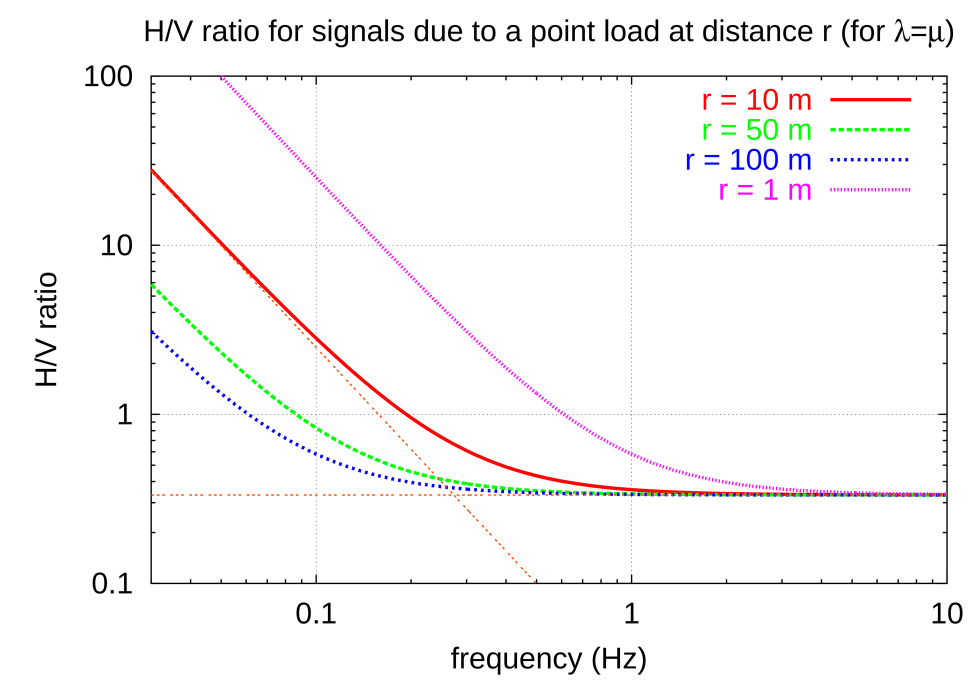

Figure 4: H/V ratio predicted by eq. (17) for a point load at distance r. Lamé's parameters are assumed to be equal ($\lambda = \mu$).

5 Propagating Rayleigh wave

The surface displacement of a plane Rayleigh wave (Fig. 5) is

$$u_z(r,t) = A(\omega)\,\sin(k(\omega)r - \omega t) \tag{20}$$

and

$$u_r(r,t) = A(\omega)\,\varepsilon(\omega)\,\cos(k(\omega)r - \omega t), \tag{21}$$

with the ellipticity $\varepsilon(\omega)$, where $\varepsilon < 0$ for prograde waves and $\varepsilon > 0$ for retrograde waves.

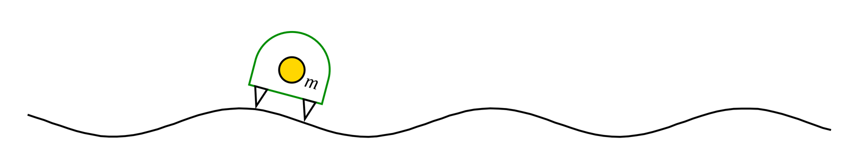

Figure 5: A propagating plane Rayleigh wave in the far-field is tilting a seismometer on the surface. The seismometer experiences an oscillating acceleration from gravity additionally to inertial acceleration.

The seismometer senses

$$a_z(r,t) = -\omega^2 A(\omega)\,\sin(k(\omega)r - \omega t), \tag{22}$$

$$a_r(r,t) = -\omega^2 A(\omega)\,\varepsilon(\omega)\,\cos(k(\omega)r - \omega t), \tag{23}$$

and

$$a_\tau(r,t) = gk(\omega)\,A(\omega)\,\cos(k(\omega)r - \omega t) \tag{24}$$

in this case.

Considering the tilt contribution from eq. (24) I obtain

$$A_{\mathrm{H/V}}(\omega) = \left|\frac{g}{\omega c(\omega)} - \varepsilon(\omega)\right|, \tag{25}$$

in the H/V analysis, where $c(\omega) = \omega/k(\omega)$ is the phase velocity. If $\varepsilon(\omega)$ and $c(\omega)$ are bounded, the H/V ratio

$$\lim_{\omega\to\infty} A_{\mathrm{H/V}}(\omega) = |\varepsilon(\omega)| \tag{26}$$

provides the ellipticity at high frequencies (as is expected) but is likely to increase with decreasing frequency at the low-frequency limit

$$\lim_{\omega\to 0} A_{\mathrm{H/V}}(\omega) = \frac{g}{\omega c(\omega)}. \tag{27}$$

Inertial and tilt contribution cancel at

$$\omega_C = \frac{g}{\varepsilon c} \tag{28}$$

for retrograde waves.
For a surface wave with $c = 2000\,\mathrm{m\,s^{-1}}$, $\varepsilon = 0.67$, and $g = 9.81\,\mathrm{m\,s^{-2}}$

$$\omega_C = 2\pi\cdot 1.2\cdot 10^{-3}\frac{1}{\mathrm{s}}. \tag{29}$$

Below 1.2 mHz the tilt effect dominates over the inertial acceleration and $A_{\mathrm{H/V}} > 1$ rises with decreasing frequency.
The frequencies for which $A_{\mathrm{H/V}} > 1$ due to the tilt contribution are not significant for our H/V studies (Fig. 6). Likewise the cancellation at ω_C cannot be observed since ω_C under realistic conditions (where phase velocity is dispersive) is smaller than the frequency of the lowest-frequency free mode (${}_0S_2$) of the earth.

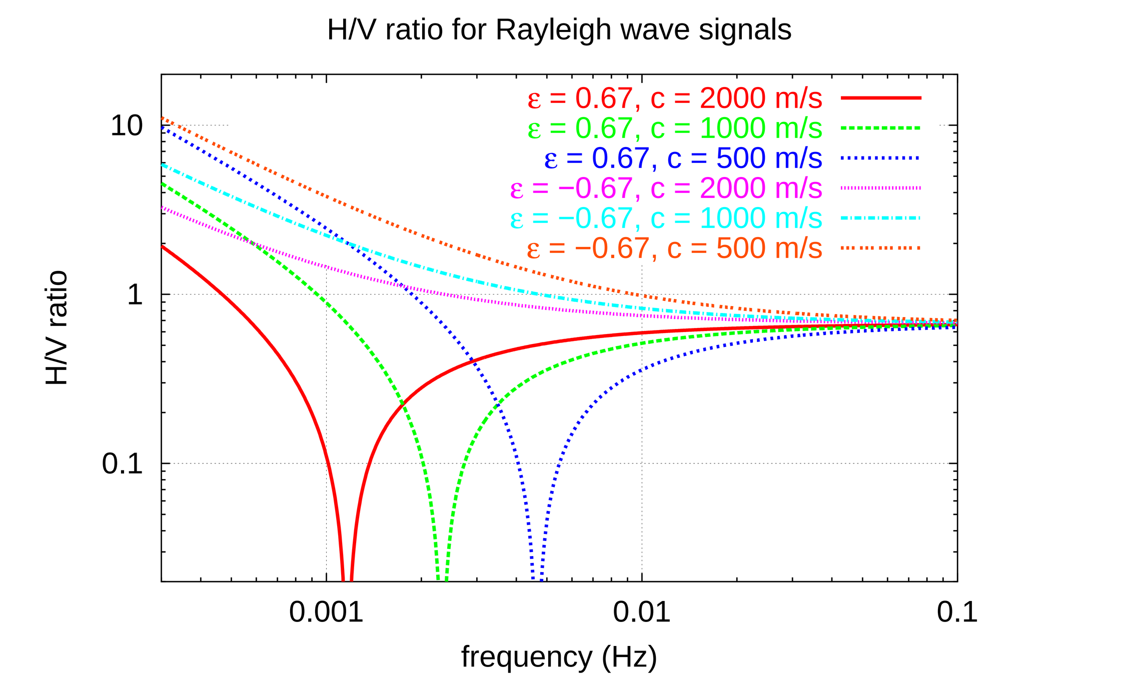

Figure 6: H/V ratio predicted by eq. (25) for surface waves of constant phase velocity c and constant ellipticity ε.

6 Conclusions

In urban environments point loads that vary with time (moving vehicles, buildings loaded by wind, etc.) must be expected to contribute to the long-period seismic signal. While the tilt contribution from Rayleigh waves is not significant in the frequency band studied with URS data, tilt due to point loads has the potential to mask surface wave ellipticity at frequencies less than 0.2 Hz. Whether this effect becomes apparent in H/V ratio depends on the relative strength of the point load compared to the amplitude of the microseisms under investigation. This and the distance-dependence of the effect may explain the strong scatter of H/V from different time windows at frequencies below 0.1 Hz in Fig. 1.

References

Ritter, J. R. R., Balan, S., Bonjer, K.-P., Diehl, T., Forbriger, T., Mărmureanu, G., Wenzel, F. & Wirth, W., 2005. Broadband urban seismology in the Bucharest metropolitan area, *Seism. Res. Lett.*, **76**(5), 574–580.

Wielandt, E., 2002. Seismic sensors and their calibration. In *New Manual of Seismological Observatory Practice*, eds. P. Bormann & E. Bergmann. GeoForschungsZentrum, Potsdam, Germany. <http://www.geophys.uni-stuttgart.de/seismometry/man_html/index.html>, <http://www.geophys.uni-stuttgart.de/downloads/Postscript-fi les>.

Ziehm, J., 2006. *Seismisches Monitoring einer Großstadt, Analyse von H/V Spektralverhältnissen*. Diplomarbeit, Geophysikalisches Institut, Universität Karlsruhe.

Zürn, W., 2003. Boussinesque-problem: Point load on an elastic halfspace. A compilation of 12 published solutions to Boussinesque's problem. Unpublished manuscript.

Acknowledgements

I'm grateful to Julia Ziehm for providing Fig. 1 and to Walter Zürn and Olivier Sèbe for inspiring discussions. URS data was recorded with the KABBA array within the framework of CRC 461.